Rapid Communications | Editors' Suggestion

Experimental realization of ultracold Yb-^{7}Li mixtures in mixed dimensions

F. Schäfer,[1,*] N. Mizukami,[2] P. Yu,[1,3] S. Koibuchi,[1] A. Bouscal,[4] and Y. Takahashi[1]

[1]*Department of Physics, Graduate School of Science, Kyoto University, Kyoto 606-8502, Japan*

[2]*Department of Physics, Faculty of Science, Kyoto University, Kyoto 606-8502, Japan*

[3]*Department of Physics, Harvard University, Cambridge, Massachusetts 02138, USA*

[4]*Département de Physique, École Normale Supérieure, PSL Research University, 24 rue Lhomond, 75005 Paris, France*

(Received 24 August 2018; published 19 November 2018)

We report on the experimental realization of ultracold ^{174}Yb-^{7}Li (boson-boson) and ^{173}Yb-^{7}Li (fermion-boson) mixtures. They are loaded into three-dimensional (3D) or one-dimensional (1D) optical lattices that are species-selectively deep for the heavy ytterbium (Yb) and shallow for the light bosonic lithium (Li) component, realizing novel mixed dimensional systems. In the 1D optical lattice the band structure of ^{173}Yb is reconstructed in the presence of ^{7}Li. Spectroscopic measurements of the ^{174}Yb-^{7}Li mixture in the 3D lattice give access to the ^{174}Yb Mott-insulator structure. Ground-state interspecies scattering lengths are determined to be $|a_{\mathrm{bg}}(^{174}\mathrm{Yb}\text{-}^7\mathrm{Li})| = (1.11 \pm 0.17)$ nm and $|a_{\mathrm{bg}}(^{173}\mathrm{Yb}\text{-}^7\mathrm{Li})| = (1.16 \pm 0.18)$ nm. The formation and characterization of an ultracold ^{173}Yb-^{7}Li mixture is a first step toward a possible realization of a topological $p_x + ip_y$ superfluid in this system.

DOI: 10.1103/PhysRevA.98.051602

I. INTRODUCTION

In recent years, the strong and interdisciplinary effort toward the realization of topological phases of matter has evolved, particularly bringing topological insulators [1] and superconductors [2] into focus. Here, chiral $p_x + ip_y$ superconductors in two dimensions (2D) are of particular interest, as the appearance of robust Majorana modes might play an important role in realizing fault-tolerant quantum computation [3]. Currently, Majorana modes are discussed in one-dimensional (1D) nanowires (see, e.g., [4,5]) and other solid-state systems; for example, Sr_2RuO_4 is shown to form a p-wave superconductor [6]. Fine-tuned control of the possible Majorana modes in these systems seems difficult, and it is highly desirable to introduce additional platforms to realize topological superfluids with good control of their properties. Ultracold atom systems could be promising candidates for this application [7]. Additionally, using multispecies systems is a familiar pathway for broadening the range of accessible physical questions and, in particular, realizing mixed-dimensional systems [8].

Following these ideas, it was shown as early as 10 years ago that a two-species Fermi gas with one species confined in a 2D plane and immersed into a three-dimensional (3D) Fermi sea of the other species could lead to $p_x + ip_y$ superfluidity facilitated by interspecies s-wave interaction [9]. Later, using Berezinskii-Kosterlitz-Thouless theory, it was found that Fermi-Bose mixtures in mixed dimensions also support this topological superfluid [10]. More detailed calculations revealed that in considering higher-order contributions, the p-wave gap can be even larger than previously expected [11]. The authors of [11] also provide detailed calculations of the transition behavior of the two-species fermionic ytterbium (^{173}Yb) and bosonic lithium (^{7}Li) system. Assuming suitable interspecies scattering lengths, critical temperatures on the order of $0.07T_{\mathrm{F}}$, with T_{F} the Fermi temperature, are predicted. Most recently, calculations including retardation and self-energy effects [12] predict similar thresholds at about $0.1T_{\mathrm{F}}$. These limits are certainly challenging. However, they are not too low for state-of-the-art experiments [13]. Indeed, the present work reports on the realization and characterization of a quantum degenerate, mixed-dimensional ^{173}Yb-^{7}Li system.

Much effort has been spent in understanding the interactions in the sister system of bosonic ^{174}Yb and fermionic ^{6}Li [14,15], where even the realization of a double superfluid was reported [16]. In this context, our work strives to expand on these efforts by reversing the roles of the particles, switching out bosonic for fermionic Yb and fermionic for bosonic Li. To complete the picture, we also report on a quantum degenerate ^{174}Yb-^{7}Li mixture.

The present Rapid Communication is organized as follows. In Sec. II, we introduce the experimental setup and details for reaching double quantum degeneracy. Section III summarizes our first characterization of the mixtures obtained, that is, the measurement of the interspecies scattering lengths (Sec. III A), the creation of a mixed-dimensional system (Sec. III B), and the high-resolution spectroscopy of the mixture in a 3D optical lattice (Sec. III C). A final discussion of the results in Sec. IV concludes our work.

II. EXPERIMENT

The experiment proceeds along similar lines as our earlier reported works [17]. In brief, a hot atomic beam is formed starting from a dual species oven heated to about 350 °C, which contains Yb and Li in natural abundances as well as enriched ^{6}Li. The isotope shifts of the optical transition frequencies are, for Yb, in the few gigahertz range and, for Li, in the 10 GHz range. Thus, isotope-selective slowing

*schaefer@scphys.kyoto-u.ac.jp

and cooling of both species is possible with only slight adjustments of the cooling laser frequencies. We first slow down Yb in a Zeeman slower operating on the strong $^1S_0$-$^1P_1$ transition followed by a magneto-optical trap (MOT) on the narrow $^1S_0$-$^3P_1$ intercombination line. In a second step, Li is slowed and trapped relying on the D_2 transition. As a comment, we note that the hyperfine splitting for the ^{7}Li($^2S_{1/2}$) ground state is, at 803.5 MHz, much larger than that for ^{6}Li at 228.2 MHz. Therefore, the inclusion of a $^2S_{1/2}(F = 1)$-$^2P_{3/2}$ repumper laser to the standard $^2S_{1/2}(F = 2)$-$^2P_{3/2}$ Zeeman slowing light is especially important for slowing sufficient numbers of ^{7}Li atoms for loading into the MOT. Compression of the MOT followed by reduction of MOT beam detunings and intensities further cools the atomic clouds. This improves phase matching for loading into our crossed far-off-resonance trap (FORT), where forced evaporative (Yb) and sympathetic (Li) cooling are performed.

For the case of a ^{174}Yb-^{7}Li mixture, we load the Yb and Li MOT for 14 and 0.5 s, respectively, which results in a typical value of 60×10^5 Yb($^1S_0$) atoms at 95 μK and 1.5×10^5 Li($^2S_{1/2}$, $F = 1$) atoms at 210 μK in the crossed FORT at the beginning of the evaporation ramp. For ^{173}Yb-^{7}Li and reoptimizing the settings of the experimental sequence, atom numbers after 20 and 0.3 s of loading are 46×10^5 for Yb at 80 μK and 0.7×10^5 for Li at 115 μK. During forced evaporation and sympathetic cooling, the crossed FORT lasers are reduced from their initial powers to the final values in individually optimized ramps within 7.65 s (9.8 s) for ^{174}Yb-^{7}Li (^{173}Yb-^{7}Li). We confirmed thermal equilibrium of the two gases during evaporation. All experiments reported in the present work were performed at low magnetic bias fields, typically a few hundreds mG, not to involve any Feshbach resonances while still providing a clear quantization axis. We note that in the work described here the ^{7}Li atoms are in the $F = 1$ state where, contrary to the $F = 2, m_F = 2$ state used in experiments with magnetic traps, the scattering length at low magnetic fields is small but positive [18], about 0.5 nm. In this situation the intraspecies interactions are repulsive and formation of a stable ^{7}Li Bose-Einstein condensate (BEC) for all atom numbers is expected. Development of phase-space density (ρ) and atom number (N) during evaporation normalized by their respective initial values, ρ_0 and N_0, for both mixtures are shown in Fig. 1. From the double logarithmic representation, we see that the initial stages of the evaporation are well described by a power law and we extract $\gamma = -d\ln(\rho/\rho_0)/d\ln(N/N_0)$, a measure for the evaporation efficiency [19], by linear fit to the data. For the ^{174}Yb-^{7}Li mixture $\gamma_{\mathrm{Yb}} = 2.9(1)$ and $\gamma_{\mathrm{Li}} = 6.5(2)$ are obtained. Similarly, in the ^{173}Yb-^{7}Li evaporation sequence $\gamma_{\mathrm{Yb}} = 2.7(1)$ and $\gamma_{\mathrm{Li}} = 12.8(6)$ are observed. The cooling efficiencies for both Yb isotopes are similar while sympathetic cooling of ^{7}Li seems to proceed more effectively in combination with ^{173}Yb. In the latter case, saturation of the ^{173}Yb phase-space density, in particular, is also visible. The generally large γ_{Li} are a result of the sympathetic cooling where the Li phase-space density is increased not at the expense of the number of Li atoms, but at the cost of the coolant species, Yb. Accordingly, γ_{Li} should be regarded as a generalized cooling efficiency rather than a single-species-picture evaporation efficiency. The observed reduction of the Li atom numbers is for the ^{173}Yb-^{7}Li mixture

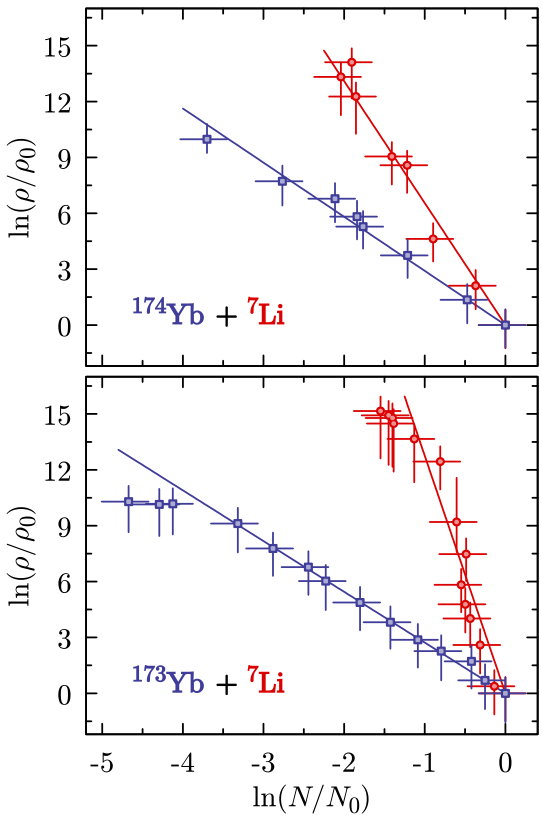

FIG. 1. The path to double quantum degeneracy in mixtures of ^{174}Yb-^{7}Li (upper panel) and ^{173}Yb-^{7}Li (lower panel). In each case, the development of the normalized phase-space density (ρ/ρ_0) and the normalized atom numbers (N/N_0) during forced evaporation and sympathetic cooling are shown as points. ρ_0 and N_0 are the respective values at the beginning of the evaporation ramp. Error bars account for uncertainties in the cloud and trap parameters. The trajectories for Yb (blue squares) and Li (red circles) can be roughly described and fitted by power laws (straight lines). See the main text for details on their interpretation.

in line with the background gas collision limited lifetime of the Li atoms in the FORT of 10–15 s. In the ^{174}Yb-^{7}Li case, where evaporation is performed faster, additional losses due to spillage of hot Li atoms from the trap seem to occur.

At the end of the evaporation ramp, due to differences in mass and a factor 2 larger polarizability of Li in the FORT light the trap frequencies for both mixtures are $(\omega_x, \omega_y, \omega_z) = 2\pi \times (38, 58, 221)$ Hz for Yb and correspondingly $2\pi \times (250, 395, 1795)$ Hz for Li, where z is in the vertical direction. (The uncertainties of those values are on the order of 10%.) The obtained quantum degenerate ^{173}Yb-^{7}Li mixture is shown in Fig. 2. We have $N \approx 62\,000$ ^{173}Yb atoms at $T = 87$ nK and from the fugacity of the Fermi gas distribution, we find by fit $T/T_{\mathrm{F}} \approx 0.4$, where T_{F} is the Fermi temperature. No optical pumping techniques have been performed on ^{173}Yb during evaporation, and we expect about equal populations of the six spin ground states. A precise determination of the condensate fraction using an unrestricted bimodal fit for the ^{7}Li cloud is difficult. We therefore opted to fix the temperature to the value obtained from the fit to the ^{173}Yb cloud and obtain $N_{\mathrm{BEC}} \approx 4200$ atoms in the BEC and $N_{\mathrm{th}} \approx 7\,400$ atoms in the

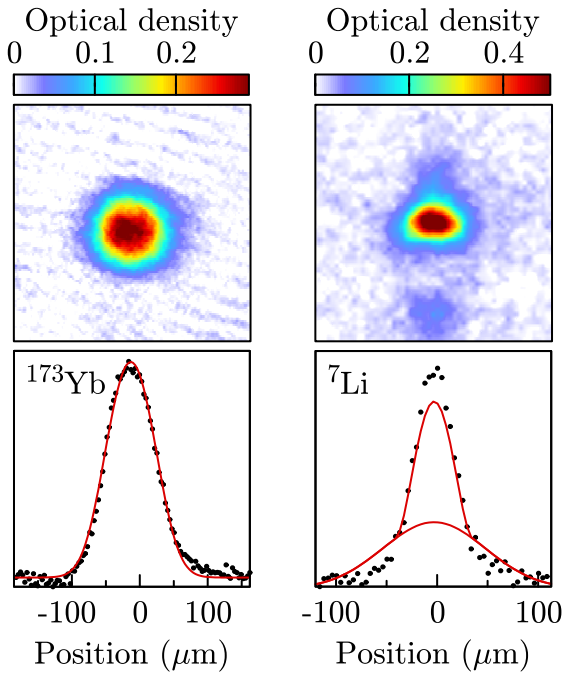

FIG. 2. A quantum degenerate mixture of ^{173}Yb (left panels) and ^{7}Li (right panels). The clouds have been imaged 15 ms (5 ms) after release from the trap for Yb (Li). The top panels show false-color representations of the obtained absorption images. The lower panels show projections of the data (points) and fit results (lines) on the horizontal axis. Fermionic ^{173}Yb was fitted by a Fermi gas distribution and bosonic ^{7}Li by a bimodal distribution (dashed line gives thermal component). The apparent discrepancy between fit and data seen in the Li projection is due to some Li atoms being ejected from the main cloud and giving rise to an additional contribution to the projection (see main text for further discussion).

thermal component for ^{7}Li, which is a condensate fraction of 0.36. In this situation a critical temperature for reaching BEC of $T_{\mathrm{C,Li}} \approx 400$ nK is expected. The time-of-flight absorption image of ^{7}Li (see right panel of Fig. 2) shows a slight fragmentation of the atomic cloud, the origin of which is not yet understood. By application of a magnetic field gradient after release of the atoms from the trap, we determined that all Li atoms are actually spin polarized in the $m_F = 0$ state and remaining field gradients cannot cause this splitting. We therefore surmise that the probable cause is some technical instability of the experiment leading to additional dynamics as the crossed FORT is being turned off. Turning our attention to the boson-boson ^{174}Yb-^{7}Li mixture (not shown), we report $N_{\mathrm{BEC}} \approx 76\,000$, $N_{\mathrm{th}} \approx 47\,000$, $T = 110$ nK for ^{174}Yb and $N_{\mathrm{BEC}} \approx 12\,000$, $N_{\mathrm{th}} \approx 14\,000$ with $T_{\mathrm{C,Li}} \approx 500$ nK for ^{7}Li, again assuming equal temperatures for both species. The condensate fractions are 0.62 and 0.46, respectively.

III. ANALYSIS AND RESULTS

Toward the long-term goal of forming a topological superfluid, three main ingredients are of particular importance [11]: (i) the creation of a fermi-boson quantum degenerate mixture at only a few nanokelvin, (ii) the formation of a mixed-dimensional system, and (iii) information on the interspecies

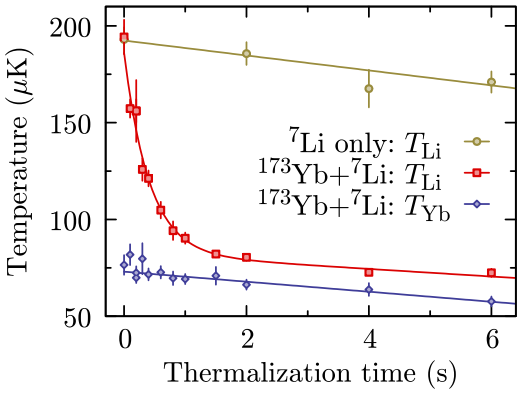

FIG. 3. Overview of experimental data to determine the ^{173}Yb-^{7}Li interspecies scattering length. After preparation of a temperature-imbalanced thermal mixture, the temperatures of Yb (blue diamonds) and Li (red squares) have been measured for thermalization times of up to 6 s. For reference, the temperature evolution of a Li-only sample has also been taken (yellow circles). While the temperature of Li in the mixture has been fitted by an exponential decay (red line), the other data have been approximated by straight line fits (blue, yellow lines). For each thermalization time, the individual temperatures have been estimated from a series of measurements at different expansion times and the error bars correspond to the uncertainties in the temperature estimation from these data.

s-wave scattering length. In the present initial survey, the experimental setup was not designed to reach the required temperatures to address the first point. Instead, we concentrate on the remaining points by both determining the interspecies background scattering length, Sec. III A, and realizing and probing two different mixed-dimensional systems, Secs. III B and III C.

A. Interspecies scattering length

Similar to earlier determinations of the ^{174}Yb-^{6}Li interspecies scattering length [20,21], we perform cross-thermalization measurements in cold, but thermal samples of ^{174}Yb-^{7}Li and ^{173}Yb-^{7}Li mixtures. The experiment starts by loading either mixture into the crossed FORT. The trapping frequencies are about $2\pi \times (137, 564, 3200)$ Hz for Yb and correspondingly $2\pi \times (917, 3785, 21285)$ Hz for Li. Trap depths of about 1 and 2 mK, respectively, are expected. After confining the sample for 3 s a steady state of 60–80 μK is reached. Then, by slight power modulation of the horizontal FORT laser beam at 9.5 kHz for 1000 ms, the Li sample is selectively heated to an isotropically equilibrated temperature of 150–200 μK. Through keeping the temperature-imbalanced mixture in the trap for a variable time before releasing it, we gain access to the temperatures by taking a series of absorption images at different expansion times and the result for the ^{173}Yb-^{7}Li case is shown in Fig. 3. During the measured thermalization times, the Yb temperature T_{Yb} is found to vary little, while the Li temperature T_{Li} quickly approaches T_{Yb}. This shows that Yb can be treated as a sufficiently large heat bath at constant temperature. We attribute the gap in final temperatures, which is accounted for in the error budget of

the data analysis, to a residual small miscalibration of the two independent imaging systems. A control measurement in which Yb is blasted by resonant $^1S_0$-$^1P_1$ light at zero holding time confirms that all cooling of the Li is due to Yb.

Standard cross-thermalization analysis [20] then gives access to the modulus of the interspecies scattering length. In the error analysis uncertainties of the atom numbers by 20%, the temperatures by 10%, and the densities by 30% are considered. For the Fermi-Bose mixture, $|a_{\rm bg}(^{173}\text{Yb-}^7\text{Li})| = (1.16 \pm 0.18)$ nm is obtained. In the corresponding experiment for the Bose-Bose mixture, we find $|a_{\rm bg}(^{174}\text{Yb-}^7\text{Li})| = (1.11 \pm 0.17)$ nm. These values should be compared to previous calculations, albeit done for different Li hyperfine states, where scattering lengths of $+1.80$ and $+1.74$ nm have been reported [22]. This shows that while good order-of-magnitude agreement is achievable, the details of the interspecies interaction potentials are quite challenging to model correctly.

B. Band structure of ^{173}Yb in a 1D optical lattice

The aspired realization of a $p_x + ip_y$ superfluid heavily depends on the formation of a novel mixed-dimensional system. Here, by means of a strong 1D optical lattice, we realize an array of 2D ^{173}Yb fermionic systems in a 3D ^{7}Li bosonic bath. The 1D optical lattice is formed by two horizontally counterpropagating laser beams [17] with wavelength $\lambda_{\rm L} = 532$ nm. To reduce the impact of the differential gravitational sag between Yb and Li of about 4 μm in this and the following experiments, a compensating beam at the same wavelength, focused slightly above the atoms, is utilized [17]. The lattice depth for Yb is set to $15E_R^{\rm Yb}$, with $E_R^{\rm Yb} = \hbar^2 k_{532}/(2m_{\rm Yb})$ being the Yb recoil energy, where $m_{\rm Yb}$ is the Yb atomic mass and $k_{532} = 2\pi/\lambda_{\rm L}$. In this situation the Li lattice depth is only $0.7E_R^{\rm Li}$, which is too shallow to support a bound state in the optical lattice, permitting the Li atoms to still freely move in 3D space. To confirm formation of the mixed-dimensional system, we then perform lattice modulation spectroscopy [23] to reveal the Yb band structure. After adiabatically ramping up the optical lattice, its depth is modulated by about $5E_R^{\rm Yb}$ for 0.3 ms and then ramped down to zero in 0.2 ms converting higher band excitations via band mapping to real momenta that can be observed after time-of-flight absorption imaging.

The process is schematically depicted in Fig. 4(a), where the first four bands of the 1D lattice for Yb are shown. The fermions initially occupy the complete first band (lower dots) and modulation of the lattice at the proper frequency leads to a particle-hole pair (filled and empty circles) between predominantly the first and third bands. Experimental data is shown in Fig. 4(b), where the real momentum distribution after time of flight is given versus the modulation frequency. The formation of particle-hole pairs is visible as areas of increased-decreased density. The black lines give the expected structure for a lattice at $14E_R^{\rm Yb}$. This indicates that the calibration of the lattice depth using Kapitza-Dirac scattering of interacting bosonic ^{174}Yb before changing the setup to work with ^{173}Yb slightly overestimated the actual potential depth. Also the weak signals at $\pm 4\hbar k_{532}$ could indicate imperfections in the band mapping procedure. A repetition of the experiment with ^{7}Li blasted away before ramping up the optical lattice (not shown) yields identical results.

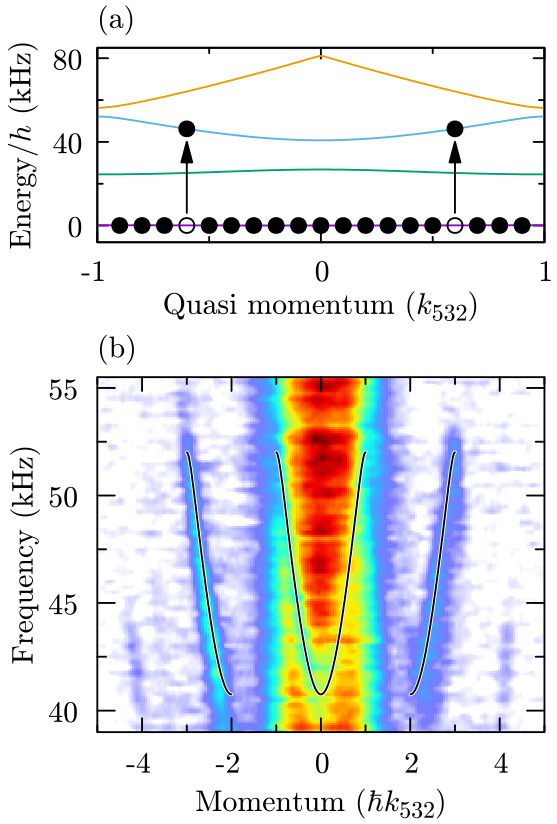

FIG. 4. Lattice modulation spectroscopy of a double quantum degenerate ^{173}Yb-^{7}Li mixture in a deep 1D optical lattice. (a) Calculated first four bands of the lattice at $14E_R^{\rm Yb}$ lattice depth (bottom purple to top orange lines). The population of the first band by Yb fermions (filled circles) and the excitation of a particle to the third band by lattice modulation (arrows), creating a hole in the first band population (open circle), are schematically indicated. (b) Experimental modulation spectroscopy data. The momentum distribution recorded by a band mapping procedure for different modulation frequencies reveals the creation of particle-hole pairs in the first and third lattice bands. The expected momentum-frequency dependence for this process is indicated (black lines). In the false-color representation light blue (dark red) corresponds to a lower (higher) momentum population probability.

C. Spectroscopy in a 3D optical lattice

We now proceed to further reduce the dimensionality of Yb in the mixed-dimensional Yb-^{7}Li systems. This can be done in almost the same manner for the ^{173}Yb-^{7}Li Fermi-Bose and the ^{174}Yb-^{7}Li Bose-Bose mixtures. For experimental ease, we choose here the ^{174}Yb-^{7}Li system and load it into a 3D cubic optical lattice at $15E_R^{\rm Yb}$, where Yb forms a Mott-insulating state while Li remains nonlocalized. In the case of ^{174}Yb, by exploiting the narrow ^{174}Yb($^1S_0 \rightarrow {}^3P_2$) transition, we are able to energetically distinguish lattice sites with different Yb occupation numbers as previously demonstrated for both a pure ^{174}Yb system [24] and the ^{174}Yb-^{6}Li mixture [15,17]. The results are summarized in Fig. 5, where a measurement in the presence of ^{7}Li (red) is compared to a situation where the Li atoms were removed from the trap just before loading the ^{174}Yb atoms into the lattice (blue). The well-resolved resonances corresponding to occupation numbers up to $n = 4$

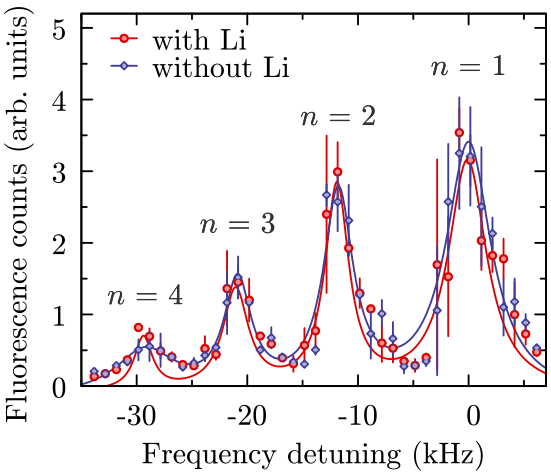

FIG. 5. Measured $^1S_0 \rightarrow {}^3P_2(m_J = 0)$ excitation spectrum (red circles) of ^{174}Yb with ^{7}Li in a 3D optical lattice at $15E_R^{\mathrm{Yb}}$. At this lattice depth, Li is not localized, while Yb forms a Mott-insulator state and atoms in lattice sites with different occupation numbers ($n = 1, 2, 3, 4$) are separated due to interatomic interaction. For comparison, the experiment was repeated with the Li atoms removed before excitation (blue diamonds). No significantly different excitation behavior is found. The lines are Lorentzian fits to the resonances.

demonstrate the successful formation of a Mott-insulating state in the presence of a ^{7}Li bosonic background gas. We also note that possible shifts of the resonance frequencies due to different interaction strengths of the Yb $^3P_2$ and $^1S_0$ states with Li have not been observed.

IV. DISCUSSION AND CONCLUSION

With the present set of experimental results, we demonstrate the realization of doubly quantum degenerate mixtures of either ^{174}Yb or ^{173}Yb and ^{7}Li. In cross-thermalization measurements the background elastic-scattering lengths have been determined. They roughly agree with earlier theoretical considerations and are generally, similar to the same mixtures involving ^{6}Li, quite small. By then loading the Fermi-Bose mixture into a 1D optical lattice, a mixed-dimensional regime has been achieved. Measurements of the ^{173}Yb band structure and of the ^{174}Yb Mott-insulator state serve to confirm formation of a mixed-dimensional state. Thus, an important step toward topological $p_x + ip_y$ superfluids has been taken. As expected, interspecies interaction effects are found to be small and enhancement mechanisms such as suitable Feshbach resonances are advantageous for reaching the required Fermi-Bose interactions. The current setup strictly relies on sympathetic cooling to reach the Li quantum degenerate regime. It is desirable to improve this situation by, e. g., implementation of Li gray molasses cooling techniques [25] and possibly the use of ^{7}Li Feshbach resonances to reduce initial temperature and to enhance evaporation efficiency. Finally, suitable lattice geometries that support the necessary bosonic excitations, while remaining experimentally feasible to realize, need to be explored.

The experiments detailed in the present work serve to establish additional quantum degenerate mixtures in the toolbox of ultracold atomic physics. It is the first large mass-imbalance Bose-Fermi system for the realization of mixed-dimensional geometries with a 3D bosonic background and a fermionic component of reduced dimensionality.

ACKNOWLEDGMENTS

This work was supported by the Grant-in-Aid for Scientific Research of JSPS Grants No. JP25220711, No. JP17H06138, No. 18H05405, and No. 18H05228; JST CREST Grant No. JPMJCR1673; and the Impulsing Paradigm Change through Disruptive Technologies (ImPACT) program by the Cabinet Office, Government of Japan.

[1] M. Z. Hasan and C. L. Kane, Rev. Mod. Phys. **82**, 3045 (2010).
[2] X.-L. Qi and S.-C. Zhang, Rev. Mod. Phys. **83**, 1057 (2011).
[3] C. Nayak, S. H. Simon, A. Stern, M. Freedman, and S. Das Sarma, Rev. Mod. Phys. **80**, 1083 (2008).
[4] V. Mourik, K. Zuo, S. M. Frolov, S. R. Plissard, E. P. A. M. Bakkers, and L. P. Kouwenhoven, Science **336**, 1003 (2012).
[5] S. M. Albrecht, A. P. Higginbotham, M. Madsen, F. Kuemmeth, T. S. Jespersen, J. Nygård, P. Krogstrup, and C. M. Marcus, Nature (London) **531**, 206 (2016).
[6] C. Kallin, Rep. Prog. Phys. **75**, 042501 (2012).
[7] N. Goldman, J. C. Budich, and P. Zoller, Nat. Phys. **12**, 639 (2016).
[8] Y. Nishida and S. Tan, Phys. Rev. Lett. **101**, 170401 (2008).
[9] Y. Nishida, Ann. Phys. (NY) **324**, 897 (2009).
[10] Z. Wu and G. M. Bruun, Phys. Rev. Lett. **117**, 245302 (2016).
[11] M. A. Caracanhas, F. Schreck, and C. M. Smith, New J. Phys. **19**, 115011 (2017).
[12] J. J. Kinnunen, Z. Wu, and G. M. Bruun, arXiv:1809.04812.
[13] N. Navon, S. Nascimbéne, F. Chevy, and C. Salomon, Science **328**, 729 (2010).
[14] W. Dowd, R. J. Roy, R. K. Shrestha, A. Petrov, C. Makrides, S. Kotochigova, and S. Gupta, New J. Phys. **17**, 055007 (2015).
[15] F. Schäfer, H. Konishi, A. Bouscal, T. Yagami, and Y. Takahashi, Phys. Rev. A **96**, 032711 (2017).
[16] R. Roy, A. Green, R. Bowler, and S. Gupta, Phys. Rev. Lett. **118**, 055301 (2017).
[17] H. Konishi, F. Schäfer, S. Ueda, and Y. Takahashi, New J. Phys. **18**, 103009 (2016).
[18] N. Gross and L. Khaykovich, Phys. Rev. A **77**, 023604 (2008).
[19] W. Ketterle and N. V. Druten, *Advances in Atomic, Molecular, and Optical Physics* (Academic, New York, 1996), Vol. 37, pp. 181–236.
[20] V. V. Ivanov, A. Khramov, A. H. Hansen, W. H. Dowd, F. Münchow, A. O. Jamison, and S. Gupta, Phys. Rev. Lett. **106**, 153201 (2011).
[21] H. Hara, Y. Takasu, Y. Yamaoka, J. M. Doyle, and Y. Takahashi, Phys. Rev. Lett. **106**, 205304 (2011).

[22] D. A. Brue and J. M. Hutson, Phys. Rev. Lett. **108**, 043201 (2012).

[23] J. Heinze, S. Götze, J. S. Krauser, B. Hundt, N. Fläschner, D.-S. Lühmann, C. Becker, and K. Sengstock, Phys. Rev. Lett. **107**, 135303 (2011).

[24] S. Kato, K. Inaba, S. Sugawa, K. Shibata, R. Yamamoto, M. Yamashita, and Y. Takahashi, Nat. Commun. **7**, 11341 (2016).

[25] A. Burchianti, G. Valtolina, J. A. Seman, E. Pace, M. De Pas, M. Inguscio, M. Zaccanti, and G. Roati, Phys. Rev. A **90**, 043408 (2014).